**Majlesi Journal of Electrical Engineering** **Vol. 11, No. 4, December 2017**

# Design of a Robust Sliding Mode Controller based on Nonlinear Modeling of Variable Speed Wind Turbine

Seyed Mahyar Mehdizadeh Moghadam[1], Alireza Khosravi [2], Seyed Mehdi Rakhtala Rostami[3]
1- Department of Electrical Engineering, University of Aliabad Katool, Golestan,Iran.
Email: mahyar.mehdizadeh67@yahoo.com (Corresponding author)
2- Faculty of Computer and Electrical Engineering, Babol Noshirvani University of Technology, Babol, Iran.
Email: akhosravi@nit.ac.ir
3- Department of Electrical Engineering, Golestan University, Golestan, Iran.
Email: sm.rakhtala@gu.ac.ir

Received: August 2017 Revised: August 2017 Accepted: August 2017

**ABSTRACT:**
In this article, the dynamic modeling of different electrical and mechanical parts of the nonlinear aerodynamics of variable speed wind turbine with Doubly Fed Induction Generator (DFIG) is addressed. Moreover, a high order robust sliding mode controller is employed to decrease the effects of the chattering phenomenon in the presence of stochastic wind model, parametric uncertainties in dynamical model, and mechanical power factor. The nonlinear robust control guarantees the performance and robust stability in order to reduce the effects of instabilities in the sliding surface and improve the turbine rotor speed variations for different angles of blade pitch. The simulation results confirm the convergence of turbine rotor speed output and the improvement of tracking error in the presence of system uncertainties.

**KEYWORDS:** DFIG, Robust sliding mode, Modeling wind turbine, Chattering.

## 1. INTRODUCTION

Fixed-speed induction generator (FSIG) and Doubly-Fed Induction Generator (DFIG) based wind turbines are two common types of wind turbines on which the control action can be implemented. Today, due to some problems such as the unadjusted wind turbine rotor speed pitches, the use of fixed speed wind turbines is not a good choice for optimal response of generator output efficiency [1, 2]. A variable speed generator based NASA/DOE Mod-2 model with two horizontal axis blades is considered in this paper [3-5], see Figures 1 and 2.

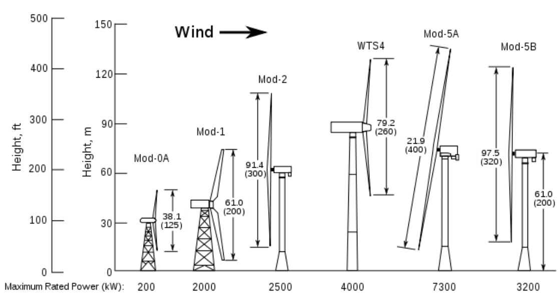


**Fig. 1.** The scale of structural design of MOD-0A to MOD-5B turbines

**Fig. 2.** NASA MMOD-2 wind turbine with a capacity of 7.5 MW in Washington Goodeno Hills, America

Due to the impact of variable speed of wind and the maximum height of 50 feet of MOE-mod2 blade center, it is difficult to control the rotor. Therefore, preventing the oscillations of mechanical stimuli (rotor and generator) is essential. To solve these problems, different control algorithms such as proportional-integral controllers [6-9], LQG controllers [10], [11], fuzzy PI controllers [12], [13], robust optimal control [14-16] and adaptive control [17] have been implemented on wind turbines. Control action is valid for a limited operating point of wind turbine. There are few studies about the nonlinear control of wind turbines using a nonlinear robust controller given the oscillating and random changes of the wind for different operating points [18], [21].

In this article, in addition to the accurate modeling of aerodynamic and mechanical parts of the turbine, a robust controller with two controlling terms is proposed for the chattering phenomenon in oscillation frequencies of wind. To reduce the chattering effect, a high order sliding mode filter is used. Given the frictions of the mechanical part of the model and various operating points of modeling uncertainties, a comparative behavior is obtained for the tracking of control objectives for robust terms with respect to different boundary layers.

## 2. WIND TURBINE NON-LINEAR CONTROL MODEL STRUCTURE

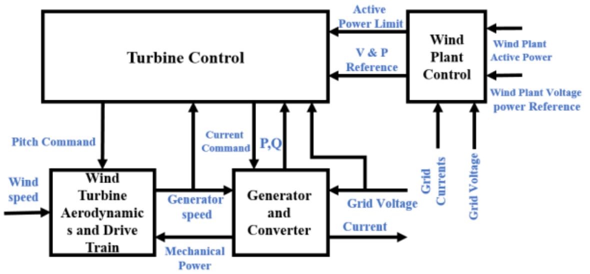


**Fig. 3**. Subsystem converting the wind model to output voltage in electrical network with nonlinear plants

In the modeling structure of wind turbine nonlinear control, various parts have been used for wind fluctuations to control the turbine generator rotor in the control objectives governing the robust procedure [22]. Table 1 shows the nominal values of the parameters governing the wind turbine system.

**Table1**. Nominal values with uncertainty and NASA MOD-2 system structure

| Uncertainty Value | | Nominal value | |
|---|---|---|---|
| $V_W$ | $0 \approx 14\ m/s$ | R | 19m |
| cp | $0.24 < cp < 0.5$ | $\omega_r$ | 2rad/s |
| $R_{f_t}$ | $0.24 < R_{f_t} < 0.5$ | $p_0$ | 100 kw |
| $J_t$ | $16kg < J_t < 18kg$ | P | $1.31\ kg/m^3$ |
| $B_t$ | $52 < B_t < 54$ | $\lambda$ | 37.5 |
| $K_t$ | $52 < K_t < 54$ | L | 0.001 |
| $K_{Q_t}$ | $1.7 < K_{Q_t} < 1.9$ | $R_f$ | 0.02 |
| $ns_r$ | 700rpm | Tg | 50kN. n |
| B | 50 | J | $16kg.m^2$ |
| K | 50 | Kw | 10 |

## 3. MODELING OF DIFFERENT PARTS OF THE WIND TURBINE

### 3.1. Wind modeling

In order to model the oscillatory behavior of the wind at any moment of time, a nonlinear differential quadratic equation with an asymptotically stable limit cycle is used [23,24] (Equation 1). The behavior of (1) shown in Fig. 5(a) does not have the stochastic nature. Hence, to create the wind fluctuations with stochastic amplitude, we apply a white noise as input dw(t) with an acceptable amplitude to the nonlinear model (Equation 3) [25]. The amplitude of wind speed variations can be changed from 1 to 14 m/s by altering the coefficient μ which is the chaos percentage of wind speed [26], [27].

$$x + \varepsilon[(\ddot{x} - x_0)^2 - \rho_0^2]\dot{x} + \mu^2(x - x_0) = 0 \qquad (1)$$

The initial conditions of the variations of wind speed and gradient of wind speed for the states of the system is as follows.

$$\rho_0^2 = x^2 + \frac{\dot{x}^2}{\mu^2} \quad , \quad (x, \dot{x}) = (x_0, 0) \qquad (2)$$

The mathematical model for the controlled wind speed system is as follows.

$$\begin{cases} \dot{x}_1(t) = x_2 + dw(t), \\ \dot{x}_2 = -\varepsilon[(\dot{x}_1 - x_1)^2 - \rho_0^2]x_2 + \mu^2(x_1 - x_0), \end{cases} \qquad (3)$$

Where ε is the mean value of wind speed, $\rho_0^2$ is the gradient of wind velocity , μ is the chaos percentage of wind speed, and $V_W = \dot{x}_2$ is the wind speed. Constant dynamic parameters of the variables $x_1$ and $x_2$ are shown in equation (4).

$$\mu = 2\pi \ , x_0 = 2 \ , \rho_0 = 0.5\varepsilon \ , \varepsilon = 10 \ , x(0) = 2 \qquad (4)$$

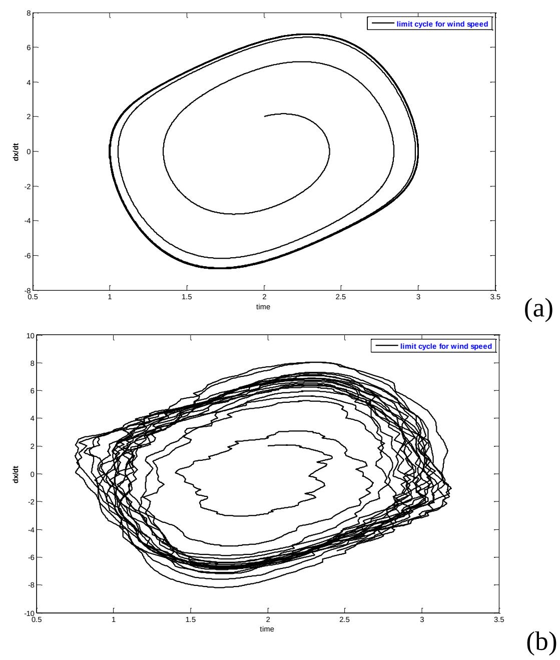


**Fig.4.** Asymptotically stable limit cycle of wind signal without chaotic and oscillatory nature (a) and wind signal with chaotic and oscillatory nature (b)

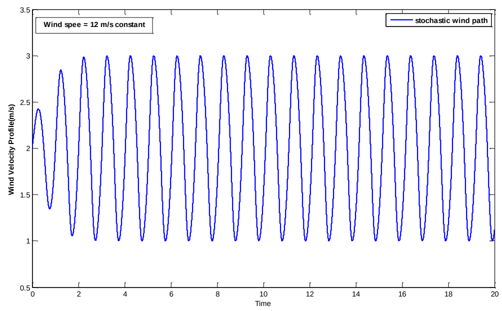


(a)

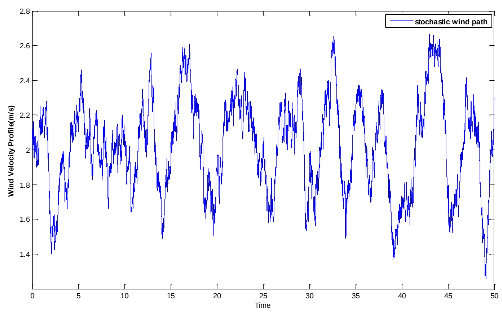


(b)

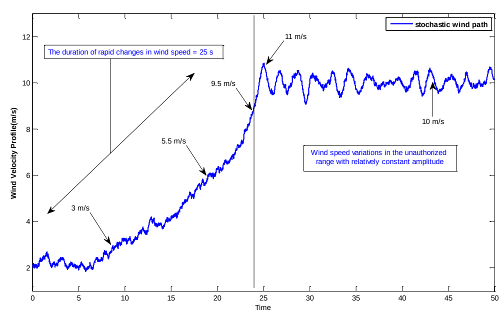


(c)

**Fig.5.** The oscillatory behavior of wind: constant speed (a), variable speed (b) and different slopes of wind speed(c)

Fig. 4 (a) demonstrates the stable limit cycle of the wind with an average speed of 10 and 10 percent of chaos. In addition, the fluctuations in the variations of the wind speed are shown in Fig. 4(b) along with the stochastic parameter dw(t). Figures 5(a) and (b) show the variations of the wind speed for two cases of constant oscillatory wind speeds of 10 and 50, while Fig. 5(c) presents the varying speed of the wind with the impact of dw(t) parameter.

### 3.2. Modeling of wind turbine rotor blade

The wind turbine rotor blade converts the torque Tm into a mechanical power for the gearbox. Given the complex dynamics of the rotor blades, the theory of the elements in the blades is required. The differential equation of the total energy $(\mathrm{dF})$ of the forces of lifting $(\mathrm{dF_L})$ and drag $(\mathrm{dF_D})$ of the blade is shown in Equation 5 [28, 29]. Equation 6 shows the energy $(P\omega r)$ obtained from the rotor with $R_{\omega r}$ and $\Omega_{\omega r}$. The power coefficient $(C_p(\lambda,\beta))$ obtained from the rotor is a function of the angle $\beta$ and $\lambda$ (Fig. 6) [30-32]. $\rho$ is the air density, $R_{\omega r}$ is the radius of the rotor. $v_W$ is the wind speed, $C_p$ represents the power coefficient of the wind turbine, $\beta$ denotes pitch angle,, $\lambda$ is the ratio of tip-speed of the blade. $c_L$ and $c_D$ are the Lift and drag coefficients and $\alpha_A$ is the angle of attack which is shown Fig 6.

$$\begin{cases} \mathrm{dF_L} = \frac{\rho}{2} v_{Wi}^2 . \mathrm{c.dr.} c_L(\alpha_A) \\ \mathrm{dF_D} = \frac{\rho}{2} v_{Wi}^2 . \mathrm{c.dr.} c_D(\alpha_A) \\ \mathrm{dF} = \frac{\rho}{2} v_{Wi}^2 . \mathrm{c.dr}[c_L(\alpha_A)\sin\alpha - c_D(\alpha_A)\cos\alpha] = \frac{\Omega_{\omega r} R_{\omega r}}{v_W} \end{cases} \quad (5)$$

$$P\omega r = \frac{1}{2}\rho\pi R_{\omega r}^2 v_W^3 . C_p(\lambda,\beta) \quad (6)$$

The following $C_p$ coefficient is considered in our simulations :( Equation 7)

$$C_p(\lambda,\beta) = 0.5\left(\frac{116}{\lambda_i} - 0.4\beta - 0.222\beta^2 - 3.33\right)e^{\frac{15.6}{\lambda_i}}, \quad \frac{1}{\lambda i} = \frac{1}{\lambda+0.08\beta} - \frac{0.035}{\beta^3+1} \quad (7)$$

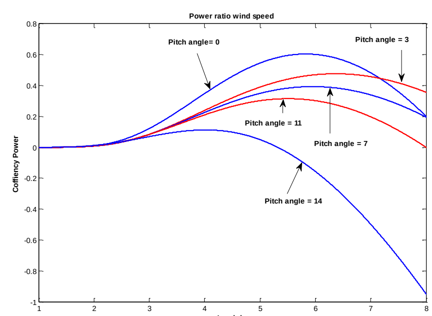


**Fig. 6.** Turbine power coefficient values with respect to different angles of turbine according to Anderson and Bose's Theory

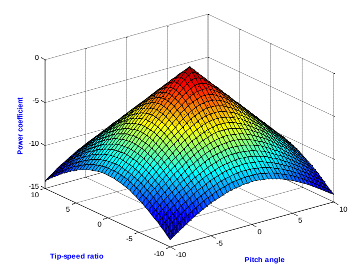


**Fig.7.** Power coefficient variations as nonlinear function of the pitch angle and the ratio of speed to the tip of the blade

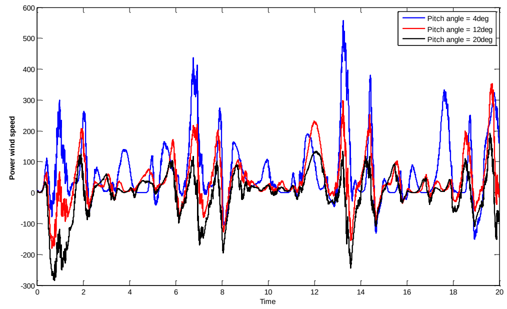


**Fig.8.** Ratio of variations in wind speed at various angles of wind turbine blades

Figures 6 and 7, demonstrate the variations in power coefficient with respect to different blade angles, blade pitch angle, and Fig. 8 presents the ratio of wind speed variations.

### 3.3. Modeling of wind turbine generator and converter

To model the wind turbine generator and converter, a model with one degree of freedom for the turbine rotor has been used (Figure 9). To stimulate the turbine blades, the wind input torque ($T_a$) is used for moving the turbine rotor with speed ($\omega_r$). Torque transmission from T and torque production in the generator shaft ($T_e$ ) are done by the gearbox. $T_e$ is the torque produced by the generator.

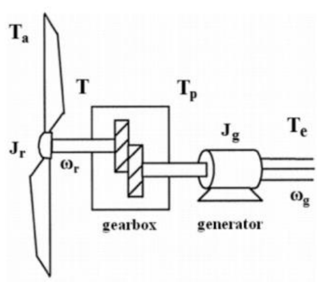


**Fig.9.** A view of the schematic of generator and converter in wind turbine power system

The equations governing the dynamics of generator and converter can be determined by Equation 8.

$$T_a + T = J_t\dot{\omega}_r + B_t\omega_r - K_t\theta_r$$
$$T_a + T_e = J_t\dot{\omega}_g + B_t\omega_g + K_t\theta_g \quad , T_p\omega_g = T\omega_r \quad (8)$$

$J_r$ and $J_g$ are the inertia moments of the turbine and the generator, respectively. $\omega_g$ and $\omega_r$ are shaft speed at the end of the turbine (turbine rotor blades) and at the end of the turbine generator (speed of generator output). $\gamma$ is the gear ratio. The analysis of equations governing $\omega_g$ and $\omega_r$ can be shown by Equation 9.

$$J_t\dot{\omega}_r + B_t\omega_r + K_t\theta = T_a - \gamma T_e$$

$$J_t\dot{\omega}_r + B_t\omega_r + K_t\theta = \frac{P_a}{\omega_r} - \gamma\frac{P_g}{\omega_g} \quad (9)$$

Initialial value $\theta$ is $\theta = \theta(t) = \int_0^t \omega_r(\tau)d\tau$ . $J_t$, $B_t$, $K_t$ and $\gamma$, are formed by Equations 10:

$$J_t = J_r + \gamma^2 J_g \ , B_t = B_r + \gamma^2 B_g \ , K_t = K_r + \gamma^2 K_g \ , \gamma = \frac{\omega_g}{\omega_r} \quad (10)$$

$$P_e = K_Q\omega_e c(I_f)$$

$$K_w = \frac{1}{2} C_p \rho\pi \frac{R_\omega{}^5}{\lambda^3} \quad (11)$$

$B_r$, $K_r$, are the rotor friction, and also, $B_g$ and $K_g$ are rotation constants. $P_e$ (Equation 11) is the electric power of generator and dependent on drive current ($I_f$), while $K_w$ is the fixed ratio of the machine. $K_Q$ and c are the flux in the generating system. The drive current can be controlled by a nonlinear dynamic system to have a nonlinear performance with magnetic unsaturated zone. For the accuracy of control function, the dynamics of turbine blade rotor and electric drive should be considered. The equations governing the dynamics of the electric dynamic system are as follows [33-34].

$$L\dot{I}_f + I_f R_f = U_f \ , I_f = (U_f - \dot{I}_f R_f)/L \quad (12)$$

With L, $I_f$ , $R_f$, and $U_f$ being the inductance of the circuit, the field current, the resistance of the rotor field, and the field control voltage, respectively. Given equations (11) and (12), the system state space equation (13) can be written as $x_1 = \theta$, $x_2 = \omega_r$ and $x_3 = \dot{\omega}_r$:

$$\begin{cases} \dot{x}_1(t) = x_2 \\ \dot{x}_2(t) = x_3 \\ \dot{x}_3(t) = \frac{1}{J_t}\left(-B_t x_2 - K_t x_1 + K_w x_2{}^2 - \gamma \times K_Q \times I_f\right) \end{cases} \quad (13)$$

The open-loop system without the effects of generator inertia is simulated for different angles and different rotor speeds. The results are shown in Figs. 10 and 11.

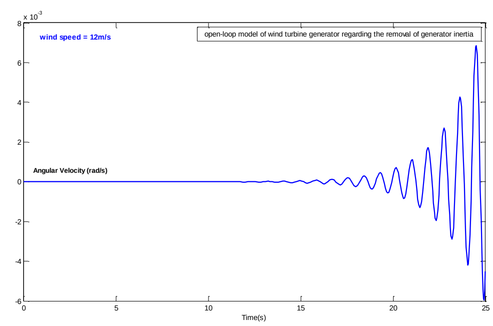


**Fig.10.** The ratio of angular velocity changes with respect to time changes for open-loop model of wind turbine generator without generator inertia

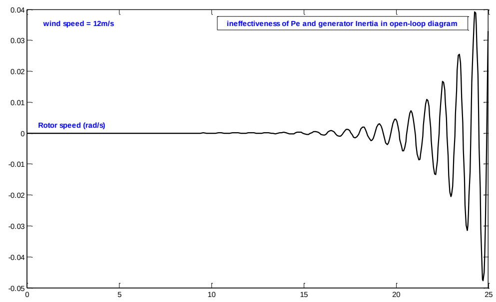


**Fig.11.** The ratio of turbine blade rotor speed changes regarding the ineffectiveness of Pe and generator Inertia in open-loop diagram

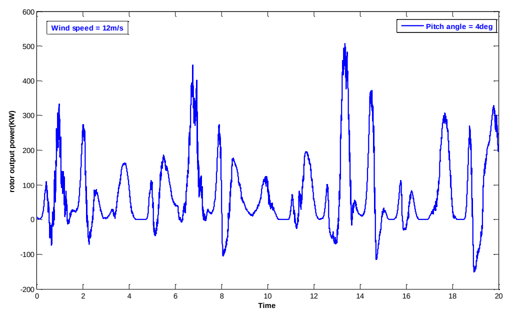


(a)

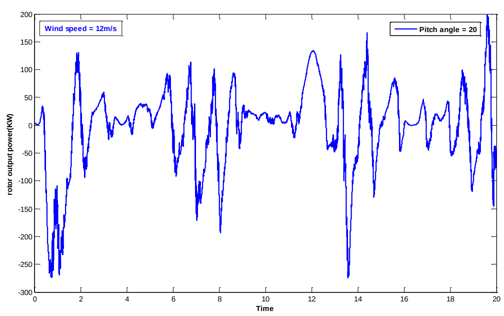


(b)

**Fig.12.** The response of the ring system depends on the variation of the output power of the rotor for the maximum permissible wind speed and the angle of 4 degrees (a) and 20 degrees (b) turbine blades

The behavior of the closed-loop system for variations of output power of the rotor for different angles is shown in Fig. 12. Generator Torque variations for different angles are presented in Fig. 13, while Fig. 14 demonstrates the simulation of the open loop system for rotor speed without the controller.

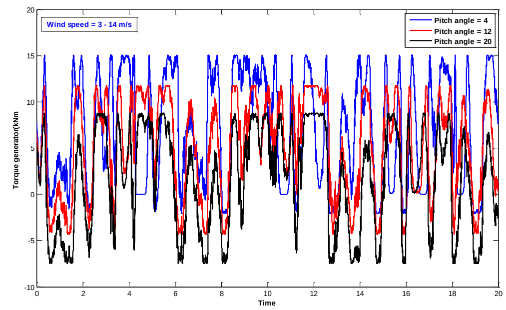


**Fig.13.** The response of the close loop changes depending on the torque of the generator for multiple desired angles

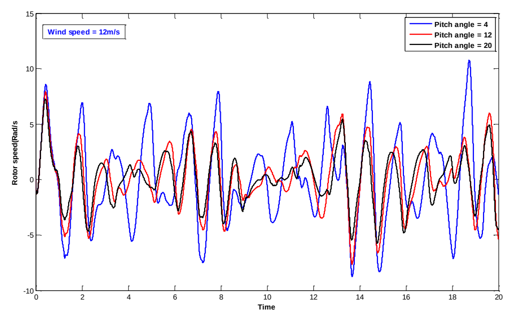


**Fig.14.** The responses to variations in the velocity of the open-loop wind turbine rotor without controller for arbitrary idle angles and constant wind speeds

## 4. DESIGN OF SLIDING SURFACES

We define S as a sliding surface according to the target signals to be tracked and wind oscillations as disturbances. As a result, we can direct the chattering to the origin using the governing equation S = 0 [35]. By placing the sliding path for relative uncertainties of the model parameters at the S, using a combination of equations, the mean of time control at the sliding surface S can be controlled even with model uncertainties and wind fluctuations (Equations 14) [35].

$$\begin{cases} e_1 = x_2 \\ e_2 = x_3 \\ e_3 = -e_1 + e_2 \end{cases} \quad (14)$$

Consider a discontinuous surface in $R$ defined by (Equations 15)

$$S = \propto_1 e_1 + \propto_2 e_2 + \propto_3 e_3 \quad (15)$$

Define the sliding surface for three state variables i = 3 and where $\propto_i \in R$, i = 1, 2, 3 are constants (Equations 16):

$$\dot{S} = \sum_{i=2}^{3} \propto_{i-1}$$

$$e_i = \propto_1 e_1 + \propto_2 e_2 + \propto_3 \left(-Be_1 - K\dot{e}_1 + Ke_1 + K_w e_1{}^2\right) + W_{v_w}(0) - \omega_{r_s}(0) = 0 \quad (16)$$

$e_1, e_2, e_3$ are Sliding surface errors for state variables for S = 0, so state equations can be considered as equation (17).

$$\begin{cases} \dot{e_1} = e_2 \\ \dot{e}_2 = e_3 \\ \dot{e}_3 = -\propto_1 e_2 \propto_2 e_3 \end{cases} \quad (17)$$

Now create a decoupled linear system for the sliding surface errors $e_2$ , $e_1$, which are effective variables in the turbine rotor speed. Define $\tilde{e} = [e_1 , e_2]^T$, then we have $\tilde{e} = A\tilde{e}$, where A is defined in Equation (18).

$$A = \begin{bmatrix} 0 & 1 \\ -\propto_1 & -\propto_2 \end{bmatrix} \quad (18)$$

$$\propto_3 \left(-ae_3 - e_2 + K_w \propto_1 - \gamma \propto_1 - e_1 K_Q \times I_f\right) + W_{v_w}(0) - \omega_{r_s}(0) - U_f = 0 \quad (19)$$

$$U_f = (\propto_2 - a)e_3 + (\propto_1 - b)e_2 + K_w \propto_1 - \gamma K_Q \times I_f(\propto_1 - e_1) + W_{v_w}(0) - \omega_{r_s}(0) \quad (20)$$

With the initial values as $\propto_1{}^* = \omega_r{}^*$ , $\propto_2{}^* = \theta^*$ , $\propto_3 = \omega_r$ , $\propto(0) = 0$ , $I_f(0) = 0$ , $\omega_r(0) = 1\text{rad/s}$ .

### 4.1. Conditions for designing the second-order sliding surface

Considering the criterion $S \neq 0$ and $S\dot{S} < 0$, the surface S = 0 is a convergence level of SS (Equation 21).

$$S\dot{S} = S[(\propto_2 - a)e_3 + (\propto_1 - 1)e_2] + S\left[\propto_3 \left(-ae_3 - e_2 + K_w \propto_1 - \gamma \propto_1 - e_1 K_Q \times I_f\right)\right] + W_{v_w}(0) - \omega_{r_s}(0) + F(\propto_m , e) \quad (21)$$

Assuming F (0)> 0 for all $\propto_m$‘ e and $t \geq 0$ (Equation 22).

$$S\dot{S} \leq |S|\left[\left|[(\propto_2 - a)e_3 + (\propto_1 - 1)e_2] + \left[\propto_3 \left(-ae_3 - e_2 + K_w \propto_1 - \gamma \propto_1 - e_1 K_Q \times I_f\right)\right] + W_{v_w}(0) - \omega_{r_s}(0) + F(0)\right| \quad (22)$$

Now, with determining the optimal values for the sliding surface for the convergence of $e_1, e_2, e_3$, we can design a robust sliding mode controller for the nonlinear model of the turbine with varying wind speed and model uncertainties. In fact, the gain $K_s$ is designed to eliminate chattering and 5% of uncertainties in system dynamics.

### 4.2. Robust sliding mode controller design based on boundary layers

The objective is to design a voltage controller ($U_f$) to keep the turbine rotor speed in the target range of controlling reference signal ($\omega_r{}^*$ with a sinusoidal and square range). Since the external disturbances of wind power require the extraction of the optimum amount of wind energy, the regulatory amount of tracking aim $\omega_r{}^*$ is defined as a time-varying input. Rules governing the control voltage robust control ($U_f$) in turbines with variable speed generator are shown in Equation 22. Uncertainty obtained from the relative changes of power factor in the range of 0.25 < CP < 0.45 is stated according to the control rate for constant speed of wind. Asymptotic stability in behavior changes of turbine rotor output speed for oscillations caused by wind is proven according to Equations 23 and 24 and regarding the nominal(Equations 23) and uncertain values (Equations 24) of mechanical and electrical components of MOE-MOD2 model generator and converter.

$$u_f = -\frac{R_f}{\gamma K_Q}\left[J\left(\dot{\propto}_1 + (\propto_1{}^* - \propto_3) + (\propto_2{}^* - \propto_2) + K_s \times \text{Sign}(\propto_1{}^* - \propto_3)\right) + B \propto_3 + K \propto_2 - K_Q \propto_3{}^2\right] \quad (23)$$

$$u_{f_t} = -\frac{R_{f_t}}{\gamma K_Q}\left[J_t\left(\dot{\propto}_1 + (\propto_1{}^* - \propto_3) + (\propto_2{}^* - \propto_2) + K_s \,\text{Sign}(\propto_1{}^* - \propto_3)\right) + B_t \propto_3 + K_t \propto_2 - K_{Q_t} \propto_3{}^2\right] \quad (24)$$

Asymptotic stability can be proven in controller dynamic error for nominal and actual models. The aim of tracking to prove asymptotic stability caused by relative uncertainties with 5% tolerance of model components can be shown by $\omega_r{}^* = 2 + \sin(t)$ and sequence of step model (Figure 16).

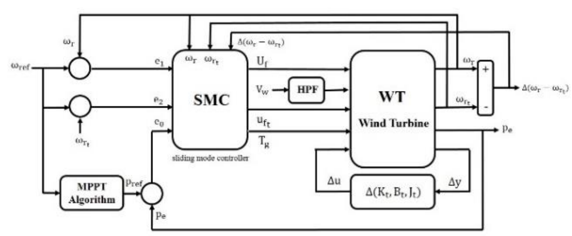


**Fig.15.** Displaying the uncertainties of nominal and actual model error and presenting a model with high order sliding mode filter to reduce the phenomenon of chattering

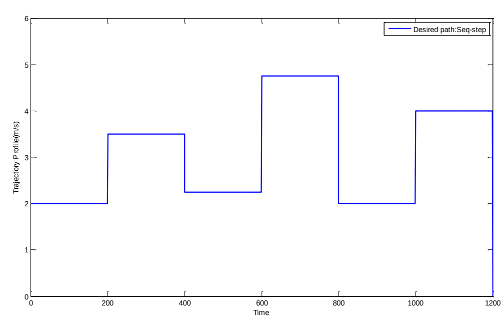


(a)

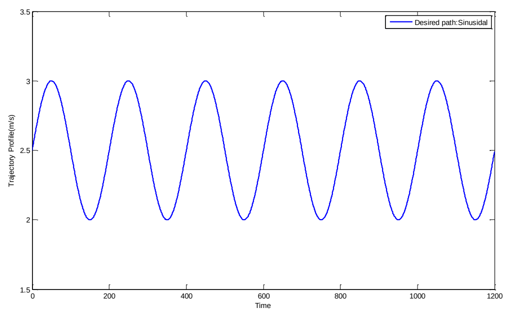


(b)

**Fig.16.** Target signal of sinusoidal (a) and (b) stepwise-ordinal tracking

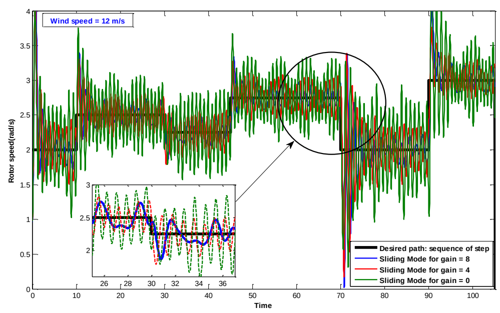


(a)

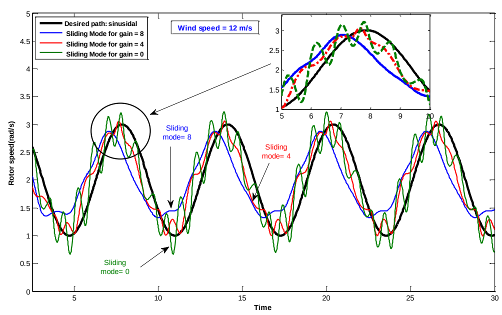


(b)

**Fig.17.** Change of rotor speed for different values of controller ($K_s$) sliding mode and 5% changes of model uncertainties, constant power factor (0.25) without controlling term and sinusoidal tracking signal (a) and stepwise-ordinal tracking signal (b)

To prevent deviant behaviors caused by changes of wind and gust speed leading to the phenomenon of chattering in oscillatory behavior of tracking the turbine rotor speed changes at the sliding mode control without filter (Figure 17), the high-order sliding mode control method is used. The second order sliding mode control method removes the input derivatives of turbine rotor speed in Equations 19 in the presence of uncertainty and oscillatory disturbance of wind and decreases the chattering phenomenon at high frequencies.

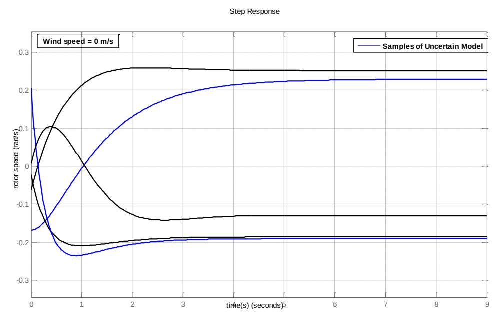


(a)

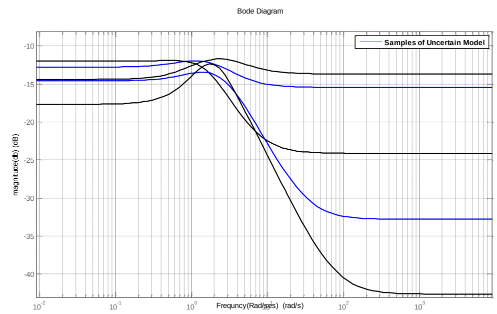


(b)

**Fig.18.** The ratio of range changes to high-order filter phase to eliminate chattering phenomenon at high frequencies of wind oscillatory behavior.(a) bode diagram and (b) step response for 5 number uncertainty

Fig. 18 presents the High Pass Filter (HPF) applied to reduce the chattering in higher frequencies.

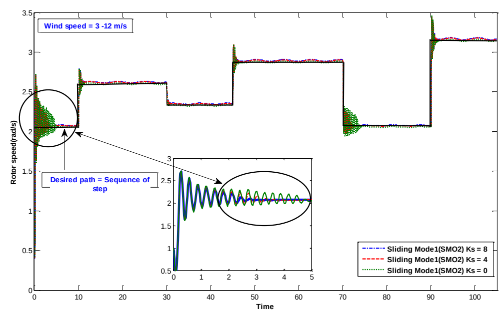


(a)

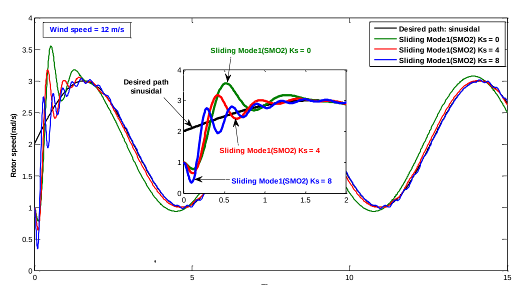


(b)

**Fig.19.** Turbine rotor speed changes for different

values of controller ($K_s$) and the use of high order sliding mode filter to reduce the phenomenon of chattering at high frequencies of wind speed changes in the presence of model dynamic error uncertainty, Cp and sinusoidal tracking signal (a) and stepwise-ordinal tracking signal (b)

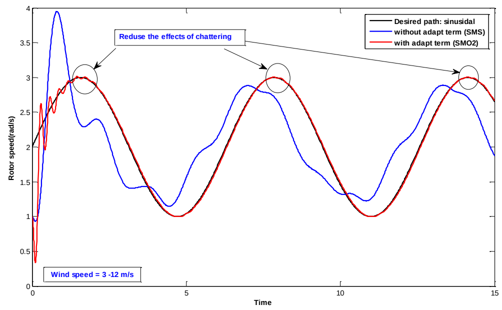


**Fig.20.** Comparison of generator rotor speed changes at two robust controlling terms with chattering effect and reducing the chattering effect by using the sliding mode filtering for wind oscillatory speed for the control rate of $K_s$ = 8, model uncertainties and Cp and sinusoidal tracking signal

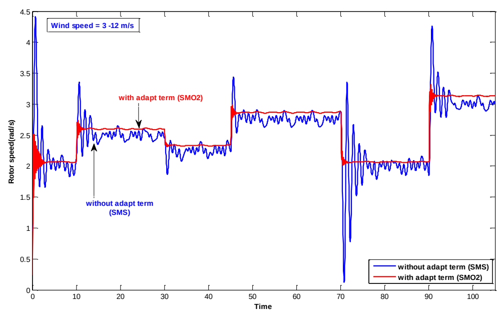


**Fig.21.** The impact of changes in terms of robust control and range of the turbine rotor speed according to the 5% target signal, uncertainty of model and fixed steps

Rotor speed variations for $U_f$ input and optimal value of $K_s$ are shown in Fig. 19. In order to show the effectiveness of the controller in eliminating chattering, we present a comparison between order 1 and higher order sliding mode controllers in Fig. 20. In Fig. 21, we show that the controller is capable of tracking the target signal in the present of variations in the uncertainties and oscillatory variations in the wind.

## 5. CONCLUSION

In this article, in addition to the accurate nonlinear modeling of electrical and mechanical parts of the horizontal axis wind turbine in the presence of model uncertainties and oscillatory behavior of wind, the optimal tracking control of wind turbine rotor was also investigated. Wind turbine generator rotor speed and generator output power were controlled optimally in the presence of uncertainties of the actual and nominal model. The results of conventional robust sliding mode controller and high order sliding mode filter were compared with each other to show the effect of chattering and reduce the effects of chattering at high frequencies of oscillatory behavior of wind and nonlinear turbine rotor speed. According to our findings, although the robust nonlinear controller with classic sliding mode is suitable in the presence of disturbance for tracking control, it causes the chattering phenomenon in oscillatory frequencies of the wind and the mechanical losses in rotor speed around the tracking signal. The use of robust sliding mode controller with high order filter removes the derivatives of turbine rotor speed input in nonlinear differential equations and decreases the chattering effect at high frequencies. The simulation results confirmed the convergence of turbine rotor speed output and the improvement of tracking error in the presence of system uncertainties.

## REFERENCES

[1] O. Anaya-Lara, **"Offshore wind energy generation, control, protection, and integration to electrical systems,"** *Wily published*, 2014.

[2] J. Fortmann, **"Modeling of Wind Turbines with Doubly Fed Generator System Dissertation,"** *University Duisburg-Essen*, 2014.

[3] L .Gary.Johnson, **"Wind Energy Systems (electronic edition) ,"** *Kansas State University published*, pp. 1-8, 2006.

[4] Boeing (2016, Oct, 1). MOD-2/MOD-5B Wind Turbines, Available: http://www.boeing.com.

[5] G. L. Johnson, **"The World Wind Energy Association,"** *USA*, Vol. 52, pp. 1–2, 2015.

[6] T. Unchim, A.Oonsivilai, **"A Study of Wind Speed Characteristic in PI Controller based DFIG Wind Turbine,"** *International Journal of Electrical, Computer, Energetic, Electronic and Communication Engineering*, Vol. 5, pp. 124–131, 2011

[7] B .Boukhezzar, L. Lupu , H .Siguerdidjanea , M .Hand. , **"Multivariable control strategy for variable speed, variable pitch wind turbines,"** *Renew Energy*, Vol.32, Issue 8, pp. 1273-1287, July 2007.

[8] GE .Van Baars, PM .Bongers, **" Wind turbine control design and implementation based on experimental models,"** in *Proc. 1992 Decision and Control IEEE Conf, Tucson, Arizona*, USA; pp. 2596-600.

[9] M .Hand, **"Variable-speed wind turbine controller systematic designs methodology: a comparison of nonlinear and linear model-based designs,"** *National Renewable Energy Laboratory NREL published*, pp.500-560. Golden, Colorado, USA, 1999.

[10] A. Kalbat, **"Linear Quadratic Gaussian (LQG) Control of Wind Turbines,"** *18th IFAC World Congress Milano. Italy*, pp.52–63, 2011.

[11] I .Munteanu, N .Cutululis, A. Iuliana, E. Ceanga, **"Optimization of variable speed wind power systems based on a LQG approach,"** *Control Engineering Practice*, Vol. 13, Issue 7, pp. 903-912 , 2005.

[12] AG .Aissaoui, A .Tahour, N .Essounbouli, F .Nollet, M .Abid, MI .Chergui, **"A fuzzy-PI control to extract an optimal power from wind turbine,"** *Energy Conversion and Management*, Vol.65, pp.688-696, 2013.

[13] H. Habibi, A. Yousefikamand, A.Sharifian, **"Power and velocity control OF wind turbines by adaptive fuzzy controller during full load operation,"** *Iranian Journal of Fuzzy Systems. Iran*, Vol. 13, No. 3, pp. 35-48, 2016.

[14] S. Bououden, M. Chadli, Hamid Reza Karimi, **"Robust Predictive Control of a variable speed wind turbine using the LMI formalism,"** *Control Conference (ECC).IEEE*, pp.190–213, 2014.

[15] FD .Bianchi, HD. Battista, RJ. Mantz, **"Wind turbine control systems: principles modelling and gain scheduling design,"** *Springer published*, pp. 10-157,2006

[16] C .Sloth, T. Esbensen, J. Stoustrup, **"Robust and fault-tolerant linear parameter varying control of wind turbines,"** *Mechatronics*, Vol. 21, pp. 645-659, 2011.

[17] Z .Song, T .Shi, C Xia, W Chen, **" A novel adaptive control scheme for dynamic performance improvement of DFIG-Based wind turbines,"** *Energy*, Vol. 38, pp. 107-118, 2012.

[18] Y. Huangfu,Ma. Ruiqing , A. Miraoui, **"Avoidance High-Frequency Chattering Second-Order Sliding Mode Controller Design: Buck Converter in Wind Power System,"** *International Journal of Antennas and Propagation. United Kingdom*, Vol. 2012, pp. 5, 2012.

[19] W. Xin, Z. Wan-li, S. Ceng, Q. Bin, **"Chattering Free Sliding Mode Pitch Control of PMSG Wind Turbine,"** *IFAC Proceedings*, Vol. 47, Issue. 3, pp. 6758-6763, 2014.

[20] M. Benbouzid, B. Beltran, Y. Amirat, G. Yao, J. Han, Herv Mangel, **"Second-order sliding mode control for DFIG-based wind turbines fault ride-through capability enhancement,"** *ISA Transactions*, Vol. 53, Issue 3, pp. 827-833, 2014.

[21] B. Torchani, A. Sellami, G. Garcia, **"Variable speed wind turbine control by discrete-time sliding mode approach,"**ISA Transactions,Vol 62, Pages 81-86 , 2016.

[22] B. Boukhezzar, H. Siguerdidjane, M. Maureen Hand, **"Nonlinear Control of Variable-Speed Wind Turbines for Generator Torque Limiting and Power Optimization,"** *J. Sol. Energy Eng*, Vol. 128, pp. 516-530, 2006.

[23] Y. Orlov, L. Aguilar, L. Acho and A. Ortiz, **"Asymptotic harmonic generator and its application to finite time orbital stabilization of a friction pendulum with experimental verification,"** *International Journal of Control*, Vol. 81, No. 2, pp. 227–234, 2007.

[24] I. Dumitrescu, **"Modeling and characterization of oscillator circuits by vanderpol model using parameter estimation,"** *Journal of Circuits Systems and Computers*, Vol. 93, pp. 98–109, 2011.

[25] W. Bier booms, P. Cheng, **"Stochastic gust model for design calculations of wind turbines"** *Journal of Wind Engineering and Industrial Aerodynamics*, Vol. 90, pp. 1237-1251, 2002.

[26] G.J.W. van Bussel, **"Constrained stochastic simulation of wind gusts for wind turbine design"**, *Duwind Delft University published*, pp.7-65, 2014.

[27] S. Kanev, T. van Engelen, **"Wind Turbine Extreme Gust Control"**, *Wind energy journal*, Vol.13, pp.18-35, 2013.

[28] A. Memon, S. R. Samo, M. Asad, and F. H. Mangi, **"Modeling of Aerodynamic Forces on the Wind Turbine Blades"**, *Journal of Clean Energy Technologies*, Vol. 3, pp.406-410, 2015.

[29] J. Fortmann, **"Modeling of Wind Turbines with Doubly Fed Generator System"**, *Dissertation University Duisburg-Essen published*, 2014.

[30] P. O. Ochieng, A. W. Manyonge**, "Mathematical analysis of tip speed ratio of a wind turbine and its effects on power coefficient",** *International Journal of Mathematics and Soft Computing*, Vol. 4, No. 1, pp. 61-66, 2014.

[31] W. Min Lin, M. Hong, **"Intelligent approach to maximum power point tracking control strategy for variable-speed wind turbine generation system"** *Energy*, Vol. 35, pp. 244-251, 2010.

[32] JG .Slootweg, SW .De Haan, H .Polinder, WL. Kling **,"General model for representing variable speed wind turbines in power system dynamics simulations",** *IEEE Trans Power System*,Vol. 18, pp. 144-151, 2003,

[33] M. Alizadeh Moghadam, R. Noroozian (C.A.) and S. Jalilzadeh, **"Modeling, Simulation and Control of Matrix Converter for Variable Speed Wind Turbine System"** *Iranian Journal of Electrical & Electronic Engineering*, Vol. 11, No. 3, pp.1-14, 2015.

[34] H. Moradi, G. Vossoughi, "Robust **control of the variable speed wind turbines in the presence of uncertainties: A comparison between H∞ and PID controllers"**, *Energy journal*, Vol. 90, pp. 1508-1521, 2015.

[35] VI. Utkin **"Sliding modes in control and optimization",** *Berlin: Springer-Verlag published*, 1992.